ISSN (Print) 1226-1750
ISSN (Online) 2233-6656
Journal of Magnetics 25(2), 164-171 (2020) https://doi.org/10.4283/JMAG.2020.25.2.164

High-Resolution Imaging Using Keyhole-Based Compressed Sensing Averaging (CSAK) Technique

Kyung-Jin Lee[1†], Chan-A Park[2†], Dae-hun Kang[3], Young-Don Son[1,2,4], Hang-Keun Kim[1,2,4], Yeong-Bae Lee[1,5,6], and Chang-Ki Kang[1,2,5,6,7*]

[1]Department of Health Sciences and Technology, Gachon Advanced Institute for Health Sciences & Technology, Gachon University, Incheon 21999, Republic of Korea
[2]Biomedical Engineering Research Center, Gachon University, Incheon 21936, Republic of Korea
[3]Department of Radiology, Mayo Clinic, Rochester, MN 55905, USA
[4]Department of Biomedical Engineering, Gachon University, Incheon 21936, Republic of Korea
[5]Neuroscience Research Institute, Gachon University, Incheon 21565, Republic of Korea
[6]Department of Neurology, Gil Medical School, Gachon University College of Medicine, Incheon 21565, Republic of Korea
[7]Department of Radiological Science, College of Health Science, Gachon University, Incheon 21936, Republic of Korea

(Received 12 March 2020, Received in final form 20 June 2020, Accepted 22 June 2020)

This study is to propose a magnetic resonance (MR) imaging technique, called as CSAK (compressed sensing averaging combined with a keyhole), and prove its possibility through *in vivo* experiment for high-resolution and fast imaging. For CSA, undersampling ratios of 25 %, 35 %, and 45 % were compared with a full k-space. Each undersampling ratio was composed of three subsets. High resolution CSAK images from the phantom and human subjects showed the increased signal-to-noise ratio (SNR) and depicted the anatomical structures more clearly. In addition, images with a 25 % undersampling ratio showed the highest SNR and reduced acquisition time by approximately 30 % relative to that of a full image. This study suggests that the proposed undersampling method for images with higher spatial and/or temporal resolution could yield better results in medical applications. Therefore, the CS-averaging technique could solve the limitations of acquiring much higher resolution images in clinical 3T MR imaging.

Keywords : fast magnetic resonance imaging, compressed sensing MRI, CS averaging, keyhole technique, SNR enhancement technique

1. Introduction

With advances in magnetic resonance imaging (MRI) technology, anatomical images have evolved into high spatial resolution images that can distinguish submillimeter structures on 1.5T and 3T MRI that are mainly used clinically [1]. However, the signal-to-noise ratio (SNR) and the contrast-to-noise ratio (CNR), which are quantifications of image quality and of contrast between tissues, respectively, tend to reduce with higher spatial resolution [1]. Moreover, a higher resolution generally requires a longer acquisition time because of acquiring a larger number of phase-encoding lines [2]. The low SNR and CNR make it difficult to discriminate anatomical structures and/or brain tissues, and the longer acquisition time makes it vulnerable to cause artifacts by motion [2]. Up to date, efforts to overcome these shortcomings have been made in a variety of ways [3-5]. Among them, averaging images can increase the SNR by reducing noise, but has not solved a long acquisition time for high-resolution images [6, 7].

The keyhole technique has been used to shorten the acquisition time by acquiring only the middle portion of phase-encoding lines in the k-space, which contains low spatial frequency information [8, 9]. The keyhole technique was first proposed as a dynamic imaging technique for obtaining real-time images, where a full k-space data is first acquired for the reference and the high frequency data of the full data is with a keyhole k-space obtained subsequently. Kang *et al.* proposed a new averaging technique by fusing the keyhole and compressed sensing

*Corresponding author: Tel: +82-32-820-4110
Fax: +82-32-820-4449, e-mail: changkik@gmail.com
†The authors are equally contributed.

(CS) techniques [10]. According to conventional Nyquist sampling theory, reconstructed images after undersampling cause aliasing, but CS method enables to restore images similar in quality to the original images, when certain conditions regarding to sparsity and incoherence are met even if the data is undersampled [11, 12]. Therefore, CS can reduce acquisition time efficiently [13, 14]. The CS-averaging technique can derive a high SNR value by averaging images with high temporal resolution using the keyhole technique and undersampling of CS [10].

Previous CS-averaging techniques were simulated by undersampling the full-sampled k-space obtained from an anthropomorphic brain phantom and adding Gaussian white noise, where a single value of 33 % was used for the undersampling ratio [10]. As a result of the simulation, the images reconstructed using the CS-averaging technique had higher SNR and temporal resolution than the fully sampled image for both the CS-averaging with multiple acquisitions (CSAM) and CS-averaging with keyhole acquisition (CSAK) techniques [10]. However, the previous study could only demonstrate the ideal noise elimination effect using adding random noise to a fully sampled k-space data rather than an undersampled k-space data acquired actually. When the CS sampling pattern is determined through undersampling from an already acquired image, the reconstructed image actually has a quality different from that of the *in vivo* images obtained with various sampling patterns. In other words, using a CS-averaging technique, it was not possible to determine whether the increased SNR value was caused by noise reduction or by the combined effect of changes in signal intensity caused by k-space undersampling. Furthermore, the previous study could not evaluate the resolution dependent CS sampling effects and the optimal k-space portions to be acquired *in vivo* experiments.

In addition, the undersampling and keyhole acquisitions should be applied to human subjects intact including physiological effects such as respiration, head or body motions that could frequently occur in human imaging studies. Therefore, in this study, we proposed that the effects of CS sampling patterns and their averaging were investigated in high-resolution imaging experiments using CSAK technique to minimize the noise induced by the physiological factors.

2. Methods

2.1. Subjects

This study was approved by the research ethics committee. In a phantom experiment, a homemade phantom

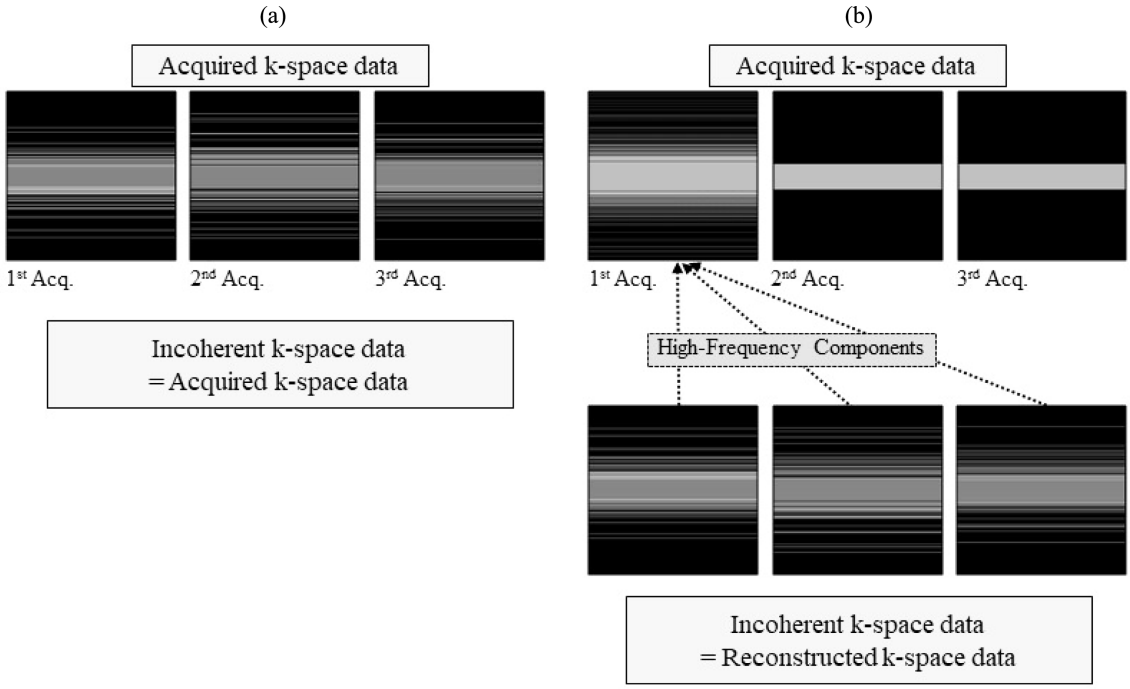

Fig. 1. The diagram of acquisition and reconstruction in k-space data using CS-averaging techniques. Each k-space data was acquired with (a) CSAM and (b) CSAK techniques. In CSAM, each k-space subset has the same number of phase-encoding lines and the acquired k-space lines are the same as those for image reconstruction. However, in CSAK, the 1st k-space subset phase-encoding lines were collected together with the high frequency components selected from 2nd and 3rd incoherent k-space subsets. For reconstruction, each subset goes through a procedure to have its own high-frequency components.

with holes of various diameters was used. Two healthy subjects participated voluntarily with an explanation of the purpose of the study and provided informed consent before starting the experiments.

2.2. Random sampling

The proposed CS-averaging technique are two categories; CSAM and CSAK. Three images for both CSAM and CSAK were acquired for averaging (i.e., number of signal averages [NSA] = 3). The CSAM technique takes three undersampled images and independently reconstructs each image through CS (Fig. 1a). On the other hand, the CSAK technique acquires the undersampled k-space data, including high frequency components, in the first acquisition and only keyhole data for the other two acquisitions. Through post-processing of the signal, the high frequency components obtained from the first acquisition are assembled with its own keyhole data to reconstruct their images through CS (Fig. 1b). For both CSAM and CSAK techniques, three reconstructed images were averaged to derive the final image.

K-space data were also obtained at three different undersampling ratios (25 %, 35 %, and 45 %) to analyze the effect of the sampling pattern on the CS-averaging reconstructed images. To prevent poor image quality caused by lack of keyhole sampling lines, a pseudo-random method was used to select the phase-encoding lines for DC components at 15 % (116 lines) of the total sampling number [12].

Because the CSAM technique has a constant number of phase-encoding lines acquired in three sets of partial k-space, the same number of samples was selected in the partial k-space according to the undersampling ratios (phase-encoding lines of 25 %, 35 %, and 45 % were 193, 268, and 346, respectively).

In the CSAK technique, 116 identical keyhole (low-frequency) phase-encoding lines were selected in common, but high-frequency phase-encoding lines for each acquisition were selected incoherently following by the previous report [12] and each subset had the maximal overlapped limit of 50 % for each other in the phase-encoding lines for high frequency components. Then, during the only first acquisition as shown in Fig. 1b, all high-frequency components were obtained depending on the undersampling ratios (i.e., phase-encoding lines of 25 %, 35 %, and 45 % were 291, 448, and 579, respectively).

2.3. Data acquisition parameters

The images were acquired using a full sample and two CS-averaging techniques from a 3T MRI scanner (Verio, Siemens, Germany). The matrix size of the images was set to 768×768. The reconstructed resolutions of phantom and human are 0.2×0.2×1 and 0.33×0.33×1.5 mm^3, respectively. A spin echo (SE) pulse sequence was used. Phantom images were measured using two echo times (TE; 15 ms for short TE and 40 ms for long TE) and two human subjects were measured using short TE (12 ms) or long TE (40 ms), respectively. Each measurement parameter is displayed in Table 1.

Table 1. MR parameters for short and long TE images.

MR Parameters	Human	Phantom
TR	460 ms	470 ms
TE (short)	12 ms	15 ms
TE (long)	40 ms	40 ms
FA	90 °	90 °
FOV	256 × 256 mm^2	154 × 154 mm^2
Imaging Resolution	0.33 × 0.33 mm^2	0.2 × 0.2 mm^2
Matrix Size	768 × 768	768 × 768
Number of Slices	10	10
Slice Thickness	1.5 mm	1.0 mm
Pixel Bandwidth	296 Hz / Px	186 Hz / Px
Partial Fourier	No	No
Elliptical Scanning	No	No

Note) TR; repetition time, TE; echo time, FA; flip angle, FOV; field-of-view.

2.4. CS Reconstruction

All the undersampled k-space data were reconstructed using the wavelet reconstructed algorithm which Lustig *et al.* implemented in MATLAB [11]. The wavelet transform was used as a sparse transform method. Based on the SNR value and clarity of the structure, the final total variation (TV) weight and L1 penalty were selected as 0.005 and 0.001, respectively. The reconstructed subset images (NSA = 3) were averaged to get a final image.

2.5. Data analysis

The reconstructed images were compared to each other by calculating the SNR value using ImageJ software [15, 16]. The SNR value was calculated as the signal in the region of interest (ROI) divided by the standard deviation (SD) of noise in the background (Fig. 2). Analysis of this study aimed at the following three topics. First, we compared the acquisition times between the CS-averaging techniques and the full sample image. Second, we analyzed image quality visually and quantitatively using SNR values. Finally, the difference between the CS-averaging acquisition methods was compared.

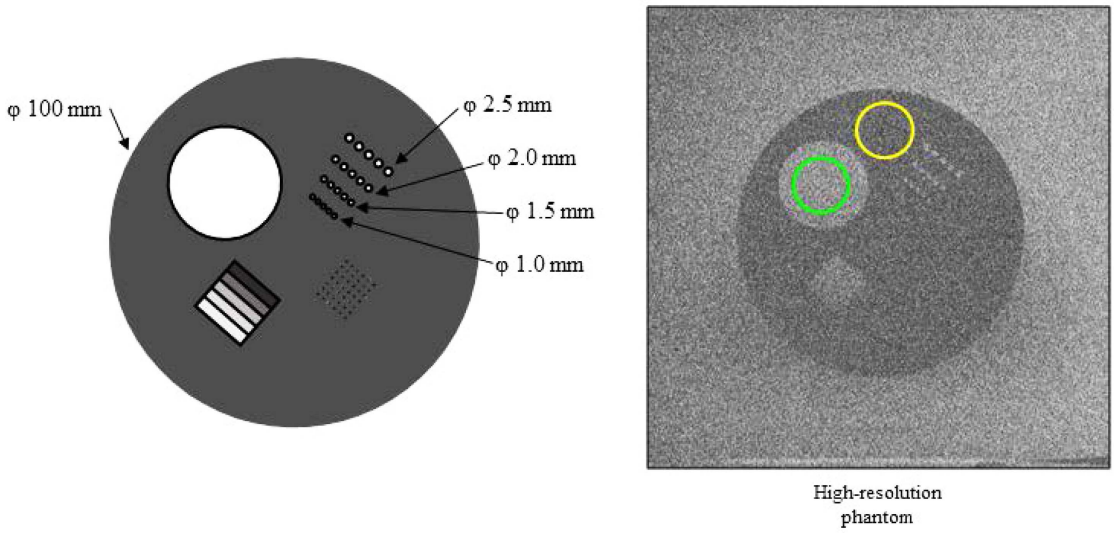

(a)

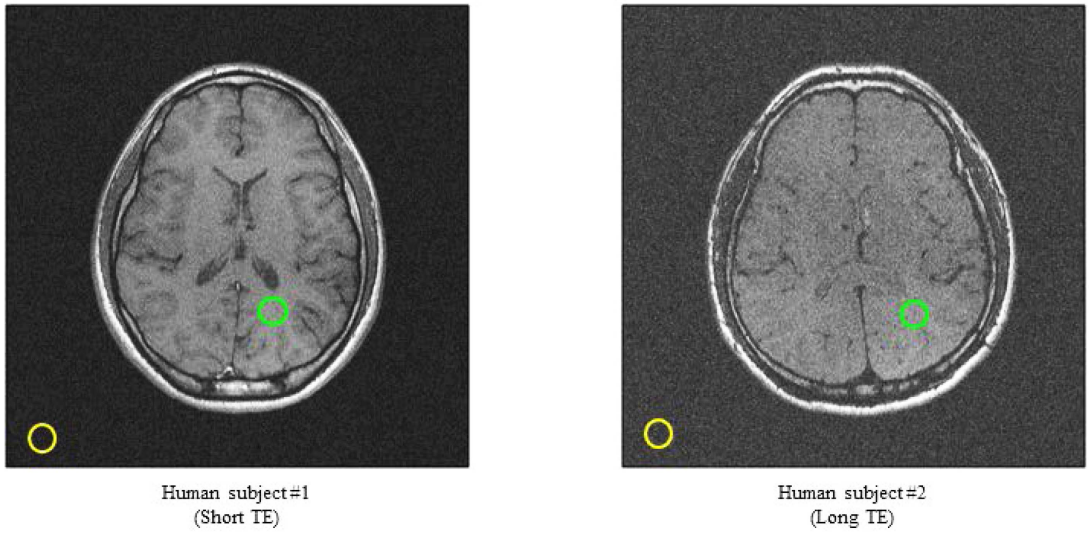

(b)

Fig. 2. (Color online) The position of ROI for the measurement of SNR. (a) A high-resolution phantom and its MR image. (b) MR images of two subjects with Short TE (left) and Long TE (right), respectively. The green circle was used for the calculation of the mean signal intensity, and the yellow circle was used for the calculation of the standard deviation of noise. ROI; region of interest, SNR; signal-to-noise ratio.

3. Results and Discussion

3.1. Acquisition time of CS-averaging technique

The CS-averaging technique focuses on averaging multiple images as well as reducing the acquisition time of each image. Because the acquisition time is determined by the number of phase-encoding lines, the undersampling ratio is exactly proportional to the acquisition time. Table 2 shows the number of phase-encoding lines and acquisition time for obtaining images using the CS-averaging technique. The CS-averaging images were calculated as the total sum of the three subsets. The acquisition time to obtain k-space subsets was the smallest when the undersampling ratio was 25 % and greatest when the undersampling ratio was 45 %. Furthermore, relative to the CSAM technique, the number of lines acquired using the CSAK technique was 10 %, 18 %, and 27 % lower at undersampling ratios of 25 %, 35 %, and 45 %, respectively.

The CS-averaging technique primarily aimed at increasing the temporal resolution by reducing acquisition time through primary undersampling. Therefore, assuming that only 25 % of the total number of phase-encoding lines and NSA=3, the CS-averaging technique requires only 75

Table 2. Acquisition time for each acquisition method and the number of phase-encoding lines in parenthesis. Note that TA was 05'56" (768 PE lines) for a full k-space sampling without averaging. TA; acquisition time, PE; phase-encoding.

Method \ Undersampling ratio	25 %	35 %	45 %
CSAM	04'33" (579)	06'18" (804)	08'03" (1,038)
CSAK	04'08" (523)	05'20" (680)	06'21" (811)

% of the full sample acquisition time. In practice, the results of the acquisition time measured during the experiments are consistent with our expectations. However, the CSAK technique, which required 69.6 % of the acquisition time of that of full sample acquisition, performed better in terms of temporal resolution than CSAM technique requiring 76.7 % of the time relative to a full sample.

The CSAK technique has a shorter acquisition time than the CSAM method because data is acquired differently. In the CSAM technique, the three subsets acquire phase-encoding lines located in the same number of different k-space positions. In contrast, the CSAK technique acquires the first subset data at once with phase-encoding lines to be shared with the second and third subsets. In both the CSAM and CSAK techniques, approximately 50 % of the phase-encoding lines to be reconstructed will overlap across the same location in different subsets.

The CSAK method acquires the overlapping lines only once in the first subset, which can then further reduce the acquisition time. This effect leads to a more efficient time reduction by increasing overlapping phase-encoding lines as the sampling rate increases. In addition, the CSAK technique will have a higher temporal resolution than CSAM technique, as the number of averaging images increases.

3.2. Image comparison between full sample and CS-averaging technique

Figure 3 shows a comparison between the full sample image and the images from the CS-averaging techniques in the phantom experiment. The CS-averaging images clearly distinguish structures better than the full sample image. While the structures of the 1~2.5 mm holes are not visible in the full sample image of the phantom, they are clearly visible in the CS-averaging technique images. The difference between the full sample and the CS-averaging images is especially obvious when considering the short TE images. The above characteristics appeared regardless of the undersampling ratio. The 1-mm structures in all

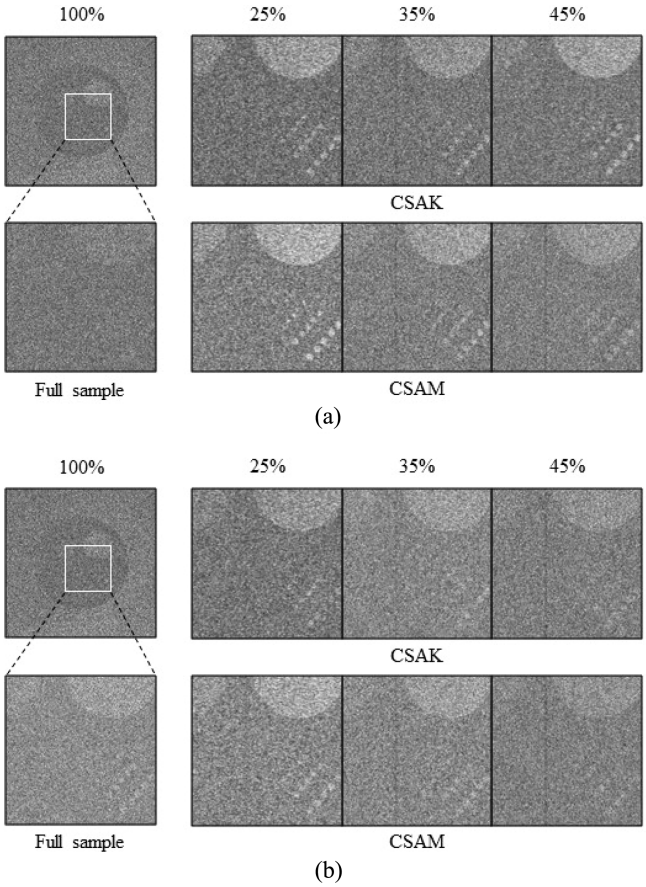

Fig. 3. Reconstructed images of the phantom with each CS-averaging technique in CSAK (top) and CSAM (bottom). The white square shows the expanded region. (a) Short TE image. (b) Long TE image. Note that the % values indicate the undersampling ratio in k-space data for the reconstructed image.

images are indistinguishable.

In human experiments, the noise seen in the full sample tended to be lower in the CS-averaging image (Fig. 4). The short TE images using CS-averaging methods showed a clear distinction between the white and gray matter. Images obtained with a lower undersampling ratio demonstrated higher contrast between the two tissues. The above features appeared regardless of the undersampling ratio.

The SNR values measured from the CS-averaging images were higher than those in the full sample images (Table 3). There was no significant difference between the CSAM and CSAK techniques, but they differed depending on the undersampling ratio. The SNR was highest when the undersampling ratio was 25 %, except for the short TE CSAK image of the phantom; the SNR of the full sample image was the lowest.

Undersampled CS-averaging images had higher SNR values than the full sample images. Structural differentiation is made possible in CS-averaging images, compared

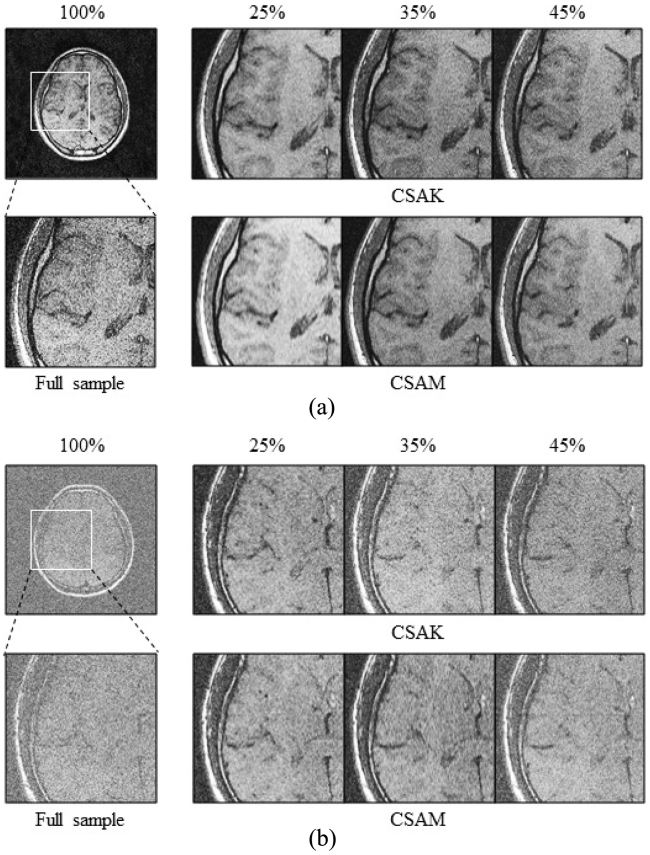

Fig. 4. Reconstructed images of the human subjects with each CS-averaging technique in CSAK (top) and CSAM (bottom). The white square shows the expanded region. (a) Short TE image. (b) Long TE image. Note that the % values indicate the undersampling ratio in k-space data for the reconstructed image.

to full sample images where structures could not be distinguished. Both increased signal intensity and decreased noise in CS-averaging images relative to those in the full sample images affected the quality of the images.

The decreased noise is an effect of averaging. When multiple images are acquired, each has different noise additively. Averaging noise reduces the noise distribution, thereby reducing the effect of noise on the resultant image. Thus, the CS-averaging image has a noise about 20 % to 50 % lower than that of the full sample image. The noise reduction effect of this CS-averaging technique has been demonstrated by previous simulation studies [10].

Another effect of the CS-averaging technique is the increase in signal intensity. In a CS-averaging technique, the reconstructed pixel size increases as the coverage narrows along the k-space phase-encoding direction. With the definition that the width to the outermost line of acquired k-space data is the width of the phase-encoding direction, the signal intensity also increases, as the pixel size increases due to k-space phase-encoding width smaller than the full sample. Therefore, these effects can be explained by the decreased signal intensity due to the increased undersampling ratio from 25 % to 45 %. As the undersampling ratio increases to 45 %, the number of lines to be acquired increases; therefore, the probability of selecting lines located at the edges increases, which increases the phase-encoding width and thus decreases the pixel size.

However, the 45 % undersampled CSAK images of the

Table 3. SNR of the reconstructed images and mean signal intensity ± SD of noise in parenthesis. SNR; signal-to-noise ratio, SD; standard deviation.

Subject	Under-sampling ratio	Short TE			Long TE		
		CSAK	CSAM	Full	CSAK	CSAM	Full
Human	25 %	15.96 (81.89±5.12)	18.42 (94.86±5.14)		9.92 (83.09±8.37)	10.09 (84.34±8.35)	
	35 %	14.09 (72.83±5.16)	13.13 (72.4±5.49)		8.57 (86.90±10.13)	10.35 (79.01±7.63)	
	45 %	12.66 (79.77±6.29)	12.30 (77.32±6.28)		7.73 (80.22±10.37)	7.91 (84.64±10.70)	
	100 %			5.43 (45.12±8.30)			4.50 (83.76±18.57)
Phantom	25 %	6.69 (120.12±17.93)	6.68 (133.16±19.33)		6.43 (117.28±18.23)	6.55 (129.77±19.80)	
	35 %	5.76 (115.25±19.98)	5.91 (122.33±20.67)		5.64 (101.66±17.99)	5.7 (122.05±21.41)	
	45 %	7.72 (122.78±16.99)	5.75 (117.92±20.49)		5.31 (114.06±21.45)	5.64 (113.98±20.18)	
	100 %			3.69 (103.57±28.03)			3.87 (104.35±26.90)

phantom were found to have SNR values similar to those of the 25 % undersampled CSAK images. This is a phenomenon that can be caused by the random k-space line selection method, and it is important to select the appropriate undersampling ratio and sampling pattern according to the resolution to correct it.

The reason for the increase in SNR values of the CS-averaging techniques is a complex consequence of the reduction in noise through averaging and increase in signal size through undersampling. In contrast to the expectation that the CSAK technique produces relatively low-quality result images because the lines of the CSAK technique were not expected to have the effects of the averaging technique (noise reduction effect) by receiving the phase-encoding lines to be shared at once, the images obtained using the CSAK and CSAM techniques did not show much difference. The similarities can be seen in the quantitative indicator of the SNR and they are simply confirmed visually. Ultimately, it can be said that noise reduction through the averaging of the keyhole lines with the low frequency components containing most of the image information contributes to better image quality than the high frequency components.

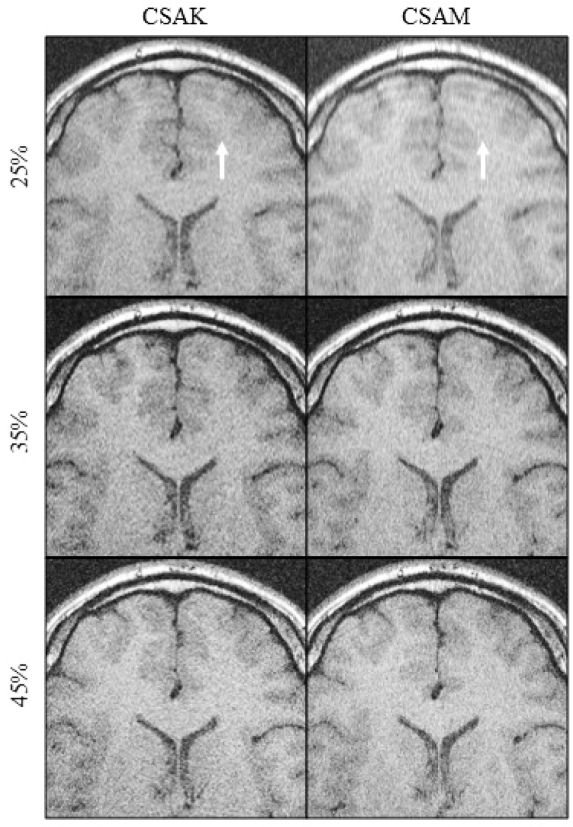

Fig. 5. The artifacts in Short TE image with each CS-averaging technique in CSAK (left) and CSAM (right). The white arrow shows the area where aliasing appears. Note that the % values indicate the undersampling ratio in k-space data for the reconstructed image.

3.3. Comparison between CSAM and CSAK techniques

Finally, we analyzed the difference between the CS-averaging techniques. There was no significant difference in SNR values, but there was a noticeable difference regarding the presence of aliasing (Fig. 5). Aliasing was greater for the CSAM method than for the CSAK technique, the most severe aliasing appeared at an undersampling ratio of 25 % and was lower at an undersampling ratio of 45 %.

The greatest difference between the CSAM and CSAK methods was the occurrence of aliasing. The reasons for the occurrence aliasing vary, but typically, it may be because of violation of Nyquist sampling theory. In CS method, undersampling is performed, which increases the probability of aliasing. Theoretically, to prevent this, the point diffusion function (PDF) is used to select the position of the phase-encoding line so that the sparse coefficients have non-interference features; however, in real experiment, a pseudo-random method using the PDF is used mainly to obtain keyhole lines, which results in aliasing due to incomplete random selection. This aliasing has a greater effect on the image as the compression ratio increases [2]. Therefore, aliasing is the most severe with an undersampling ratio of 25 % leading to a few phase-encoding lines.

However, the first data subset in the CSAK technique receives more phase-encoding lines than in the CSAM technique, because it receives all lines at once that will be shared with the second and third subsets. The number of lines in the first subset is 291, 448, or 579 for 25 %, 35 %, and 45 % undersampling ratios, respectively. This is 1.5 times higher than CSAM technique, that is, 193, 268, and 346 lines, respectively.

Eventually, the CSAK technique would only marginally violate the Nyquist sampling theory because it has more phase-encode lines in the first image than the CSAM technique, and the effect of aliasing would be greatly reduced as the k-space data with this information were shared with the remaining data subsets.

In contrast of no aliasing in the phantom simulation in the previous study [10], the present study showed aliasing in the images of the phantom. This proves that this aliasing of the CS-averaging technique is a phenomenon that occurs in the signal acquisition stage. However, the CSAK images also show a relative decrease in this phenomenon.

4. Conclusion

In this study, high-resolution phantom imaging experiments were conducted to analyze the effect of CS sampling patterns and their averaging, especially on signal intensity. Furthermore, these undersampling and keyhole acquisitions were applied to human subjects to consider physiological effects such as their movement that could frequently occur in human imaging studies. Moreover, the quality of the images depending on the various undersampling ratios was compared.

In conclusion, this study examined the increased effects of CS-averaging techniques on the SNR and the possibility of obtaining high-resolution images through *in vivo* experiments. The result demonstrated that the fully sampled image had a huge resolution loss due to inadequate SNR when the images were acquired at such an unusually high spatial resolution. Compared to full sample images, the reduced acquisition time of CS-averaging techniques can be a solution to improving low temporal resolutions, which is a limit of conventional averaging techniques. Thus, these results of *in vivo* experiments demonstrate that better quality images can be obtained even at higher resolutions and lower undersampling ratios than those reported in previous studies. The effect of the CS-averaging techniques for SNR increment was influenced not only by the averaging effect of k-space data, but also by the reduction in the coverage of k-space that occurs due to undersampling. It also showed that in the clinical application of CSAK technique, it has a lower acquisition time and the degraded aliasing effect rather than CSAM technique. This property could be comparable to images obtained at higher field MRI such as 7T MRI which has well known to provide the high resolution and SNR images. Furthermore, these fast imaging techniques can be a necessary imaging technique for acquiring images of various patients, for example with claustrophobia and tremor, as well as children sensitive to movement when acquiring images similar with the other previous studies [17, 18].

However, in further studies the sampling patterns to demonstrate the mechanism of aliasing using the pseudo-random method and causes of aliasing in the CSAM and CSAK techniques should be still examined. Moreover, further studies should suggest criteria for selecting one of the CS-averaging methods for MRI images with a lower aliasing rate. Finally, studies should be conducted to reduce the aliasing due to limitations of the undersampling patterns of MR images by using state-of-the-art algorithms to derive the appropriate pattern and rate.

Acknowledgments

Funding: This research was supported by the National Research Foundation of Korea (NRF) grant funded by the Korea government (MSIT) (2020R1A2C1004355) and the Gachon University Gil Medical Center (Grant number: 2018-11).

References

[1] J. H. Duyn, P. van Gelderen, T.-Q. Li, J. A. de Zwart, A. P. Koretsky, and M. Fukunaga, Proc. Natl. Acad. Sci. U.S.A. **104**, 11796 (2007).
[2] S. D. Sharma, C. L. Fong, B. S. Tzung, M. Law, and K. S. Nayak, Invest Radiol. **48**, 638 (2013).
[3] J. Moore, M. Drangova, M. Wierzbicki, and T. M. Peters, in MICCAI (2003).
[4] E. Plenge, D. H. J. Poot, M. Bernsen, G. Kotek, G. Houston, P. Wielopolski, L. van der Weerd, W. J. Niessen, and E. Meijering, Magn. Reson. Med. **68**, 1983 (2012).
[5] K. P. Pruessmann, M. Weiger, M. B. Scheidegger, and P. Boesiger, Magn. Reson. Med. **42**, 952 (1999).
[6] C. J. Holmes, R. Hoge, L. Collins, R. Woods, A. W. Toga, and A. C. Evans, J. Comput. Assist. Tomogr. **22**, 324 (1998).
[7] C. Eichner, S. F. Cauley, J. Cohen-Adad, H. E. Möller, R. Turner, K. Setsompop, and L. L. Wald, Neuroimage **122**, 373 (2015).
[8] J. J. van Vaals, M. E. Brummer, W. T. Dixon, H. H. Tuithof, H. Engels, R. C. Nelson, B. M. Gerety, J. L. Chezmar, and J. A. den Boer, J. Magn. Reson. Imaging **3**, 671 (1993).
[9] R. A. Jones, O. Haraldseth, T. B. Müller, P. A. Rinck, and A. N. Oksendal, Magn. Reson. Med. **29**, 830 (1993).
[10] C.-K. Kang and H.-K. Kim, Appl. Magn. Reson. **47**, 823 (2016).
[11] M. Lustig, D. L. Donoho, J. M. Santos, and J. M. Pauly, IEEE Signal Processing Magazine **25**, 72 (2008).
[12] M. Lustig, D. Donoho, and J. M. Pauly, Magn. Reson. Med. **58**, 1182 (2007).
[13] H. Jung, K. Sung, K. S. Nayak, E. Y. Kim, and J. C. Ye, Magn. Reson. Med. **61**, 103 (2009).
[14] U. Gamper, P. Boesiger, and S. Kozerke, Magn. Reson. Med. **59**, 365 (2008).
[15] T. J. Collins, BioTechniques **43**, 25 (2007).
[16] M. Abramoff, P. Magalhães, and S. J. Ram, Biophotonics International **11**, 36 (2004).
[17] S. R. Lee, Y. J. Kim, and K. G. Kim, J. Korean Med. Sci. **33**, (2017).
[18] Y. H. Sung and E. Y. Kim, Radiology **292**, 267 (2019).